2010

Controlled release of neurotrophin-3 and platelet-derived growth factor from fibrin scaffolds containing neural progenitor cells enhances survival and differentiation into neurons in a subacute model of SCI

Philip J. Johnson
Washington University in St Louis

Alexander Tatara
Washington University in St Louis

Alicia Shu
Washington University in St Louis

Shelly E. Sakiyama-Elbert
Washington University School of Medicine in St. Louis

Cell Transplantation, Vol. 19, pp. 89–101, 2010

0963-6897/10 $90.00 + .00
DOI: 10.3727/096368909X477273
E-ISSN 1555-3892
www.cognizantcommunication.com

Controlled Release of Neurotrophin-3 and Platelet-Derived Growth Factor From Fibrin Scaffolds Containing Neural Progenitor Cells Enhances Survival and Differentiation Into Neurons in a Subacute Model of SCI

Philip J. Johnson,* Alexander Tatara,* Alicia Shiu,* and Shelly E. Sakiyama-Elbert*†‡

*Department of Biomedical Engineering, Washington University, St. Louis, MO, USA
†Division of Plastic and Reconstructive Surgery, Department of Surgery,
Washington University School of Medicine, St. Louis, MO, USA
‡Center for Materials Innovation, Washington University, St. Louis, MO, USA

A consistent problem with stem/neural progenitor cell transplantation following spinal cord injury (SCI) is poor cell survival and uncontrolled differentiation following transplantation. The current study evaluated the feasibility of enhancing embryonic stem cell-derived neural progenitor cell (ESNPC) viability and directing their differentiation into neurons and oligodendrocytes by embedding the ESNPCs in fibrin scaffolds containing growth factors (GF) and a heparin-binding delivery system (HBDS) in a subacute rat model of SCI. Mouse ESNPCs were generated from mouse embryonic stem cells (ESCs) using a 4–/4+ retinoic acid (RA) induction protocol. The ESNPCs were then transplanted as embryoid bodies (EBs, 70% neural progenitor cells) into the subacute model of SCI. ESNPCs (10 EBs per animal) were implanted directly into the SCI lesion, encapsulated in fibrin scaffolds, encapsulated in fibrin scaffolds containing the HBDS, neurotrophin-3 (NT-3), and platelet-derived growth factor (PDGF), or encapsulated in fibrin scaffolds with NT-3 and PDGF with no HBDS. We report here that the combination of the NT-3, PDGF, and fibrin scaffold (with or without HBDS) enhanced the total number of ESNPCs present in the spinal cord lesion 2 weeks after injury. In addition, the inclusion of the HBDS with growth factor resulted in an increase in the number of ESNPC-derived NeuN-positive neurons. These results demonstrate the ability of fibrin scaffolds and the controlled release of growth factors to enhance the survival and differentiation of neural progenitor cells following transplantation into a SCI model.

Key words: Spinal cord injury (SCI); Neurotrophin-3 (NT-3); Platelet-derived growth factor (PDGF); Controlled release; Embryonic stem cell-derived neural progenitor cell (ESNPC)

INTRODUCTION

Spinal cord injury (SCI) is a devastating condition that results in significant damage to descending and ascending axonal networks, glial and neuronal cell necrosis, and the formation of an environment that is inhibitory to axonal regeneration (13,22). Only limited spontaneous regeneration and functional recovery occurs after SCI. One mechanism for spontaneous recovery that has been characterized in rodents is regeneration of damaged supraspinal cord axons over short distances to form local connections with surviving spinal cord interneurons (3,4,9). It is hypothesized that the formation of these local connections facilitates the long-distance relay of supraspinal signals and restores limited function following injury. The effectiveness of this spontaneous mechanism for regeneration may be limited in the case of substantial loss of spinal cord interneurons at the site of injury and by an environment that inhibits the ability of damaged supraspinal axons to regenerate over long distances (3).

As a treatment for SCI, stem cells offer a potential cell source to replace lost cells. Neural progenitor cells (NPCs) are stem cells that are restricted to differentiate into one of the three major neural cell fates (10). The limited differentiation potential of NPCs into only neural cell types has made them an attractive target for SCI treatment. They can be obtained from sites of neurogenesis in the fetal or adult brain (e.g., SVZ) and spinal cord (24), or derived from embryonic stem cells (ESCs) through induction in culture (2). Prior studies of NPCs

Received April 10, 2009; final acceptance October 1, 2009. Online prepub date: October 9, 2009.
Address correspondence to Shelly Sakiyama-Elbert, Department of Biomedical Engineering, Washington University, Campus Box 1097, One Brookings Drive, St. Louis, MO 63130, USA. Tel: (314) 935-7556; E-mail: sakiyama@wustl.edu

transplanted into the injured spinal cord have found that their survival is often poor and that the cells predominately differentiate into glia (7,8,21). One hypothesis for the predisposition for glial differentiation following transplantation into the injured spinal cord was given by Cao et al., who have shown that the environment in the spinal cord following injury inhibits differentiation of NPCs into a neuronal fate (6). The differentiation of transplanted NPCs into astrocytes may be problematic because reactive gliosis is believed to be an inhibitor of regeneration (23,26). SCI treatments utilizing stem cells are currently limited by poor cell survival and uncontrolled differentiation in part as a result of the transplantation environment.

Nakamura et al. showed that given a favorable environment (injured neonatal spinal cord), transplanted NPCs can survive, integrate with host tissue, and differentiate into neurons and oligodendrocytes (25). Furthermore, they found that repopulation of the injured spinal cord with neurons and oligodendrocytes contributed significantly to plasticity and regeneration that resulted in functional recovery. While the environment of the injured neonatal spinal cord, which is conducive to regeneration, differs significantly from the more inhibitory adult spinal cord (7), these results illustrates that NPC-derived neurons and oligodendrocytes can have a positive effect on functional recovery. The survival of transplanted NPCs following SCI can be enhanced using GF delivered over 7 days from an osmotic pump (18). In this study, the survival of transplanted cells was enhanced but the transplanted NPCs adopted a glial fate. The difficulty of promoting the survival of transplanted NPCs and controlling their differentiation into neurons has led our group to investigate a novel scaffold for transplantation.

The current study evaluated a method to enhance ESNPC viability and direct their differentiation into a population of neurons and oligodendrocytes following transplantation into a subacute model of SCI (17). Embryonic stem cell-derived neural progenitor cells (ESNPCs) were derived from mouse ESCs using a 4–/4+ RA induction protocol (2). The ESNPCs were encapsulated in fibrin scaffolds with or without a heparin-binding delivery system (HBDS) that allowed for the controlled delivery of neurotrophin-3 (NT-3) and platelet-derived growth factor (PDGF) (27). Fibrin scaffolds containing the HBDS have been shown to control the release of NT-3 and PDGF in vitro (32). At 2 weeks following transplantation, the treated spinal cords were harvested and evaluated for ESNPC viability, differentiation, and host spinal cord response. We report here that transplanting ESNPCs within fibrin scaffolds containing growth factor (GF) enhanced the total number of donor-derived cells present in the spinal cords at 2 weeks after transplantation. Furthermore, the addition of the HBDS to the fibrin scaffolds and GF resulted in an increase in the number of ESNPC-derived NeuN-positive neurons.

MATERIALS AND METHODS

Embryonic Stem Cell Culture and Embryoid Body Formation

CE3 mouse ESCs genetically engineered to express green fluorescent protein (GFP) under the β-actin promoter were obtained from D. Gottlieb and were cultured in T25 flasks (Fisher, Pittsburgh, PA) coated with a 0.1% gelatin solution (Sigma, St. Louis, MO) in the presence of 1000 U/ml leukemia inhibitory factor (LIF; Chemicon, Temecula, CA) and 10^{-4} M β-mercaptoethanol (BME; Invitrogen, Grand Island, NY) to maintain their undifferentiated state. These cells were grown in complete media consisting of Dulbecco's modified Eagle media (DMEM) (Invitrogen) supplemented with 10% newborn calf serum (NBCS; Invitrogen), 10% fetal bovine serum (FBS, Invitrogen), and 0.3 M of each of the following nucleosides: adenosine, guanosine, cytosine, thymidine, and uridine (Sigma) and passaged at a ratio of 1:5 every 2 days.

Undifferentiated ESCs were induced to form EBs containing ESNPCs using a 4–/4+ RA induction protocol (2). ESCs were cultured in 100-mm petri dishes (Fisher) coated with a 0.1% agar solution (MidSci, Saint Louis, MO) in complete media in the absence of LIF and BME for 4 days. RA (500 nM; Sigma) was added to the complete media for the final 4 days of culture. The media was changed every other day during induction. The resulting EBs contained 70% nestin-positive NPCs (31).

Tissue Engineered Fibrin Scaffold Preparation

All materials were purchased from Fisher Scientific (Pittsburgh, PA) unless otherwise noted. Fibrin scaffolds were made as described previously by mixing the following components: human plasminogen-free fibrinogen containing Factor XIII (10 mg/ml, Sigma), $CaCl_2$ (5 mM), and thrombin (12.5 NIH U/ml, Sigma) in Tris-buffered saline (TBS, 137 mM NaCl, 2.7 mM KCl, 33 mM Tris, pH 7.4) (27). The bidomain affinity peptide for the HBDS, denoted ATIII, was synthesized by standard solid phase Fmoc chemistry as described previously (27). In scaffolds containing the HBDS, ATIII peptide (0.25 mM) and heparin (6.25 μM, Sigma, sodium salt from porcine intestinal mucosa) were added to the fibrin polymerization mixture. In scaffolds containing ESNPCs, the EBs were added directly to the polymerization mixture prior to polymerization. Polymerized fibrin scaffolds (10 μl in volume) were formed by ejecting the polymerization mixture from a 20-μl pipette tip such that a sphere of the mixture formed on the tip of

the pipette. The sphere was then allowed to polymerize on the pipette tip for 5 min prior to implantation into the injury site. A second 20-µl polymerization solution devoid of EBs was then injected directly onto the sphere already in the injury site and allowing it to polymerize in the lesion site and stabilize the sphere in the injury site.

In Vivo Studies: Dorsal Hemisection Subacute SCI and Scaffold Implantation

All experimental procedures on animals complied with the Guide for the Care and Use of Laboratory Animals and were performed under the supervision of the Division of Comparative Medicine at Washington University. Long-Evans female rats (250–275 g, Harlan, Indianapolis, IN) were anesthetized using 4% isoflurane gas (Vedco Inc., St Josephs, MO). The skin and muscle overlying the spinal column were incised and dissected away from the spinal column. Clamps attached to the spinous processes and a rigid frame was used to immobilize the spinal column. A dorsal laminectomy was performed using fine rongeurs at level T-9 to expose the spinal cord. A lateral slit in the dura was made, and microdissection scissors mounted to a micromanipulator were lowered into the spinal cord 1.2 mm from the dorsal spinal cord surface. Using the microdissection scissors, a lateral incision was made to form a complete dorsal hemisection of the spinal cord. Finally the microdissection scissors were run through the incision to assure the hemisection was complete. The cord was then covered with a piece of artificial dura (generous gift of Synovis Surgical Innovations, St. Paul, MN), the muscles were sutured with degradable sutures, and the skin was stapled close. Two weeks following initial injury the lesion was reexposed, and scar tissue was removed from the wound site of control and experimental groups in preparation of fibrin scaffold transplantation.

A 2-week study was performed to evaluate the survival, differentiation, and host response to ESNPCs transplanted in tissue engineered fibrin scaffolds. ESNPCs were transplanted as EBs based on previous work (30). Each EB contains approximately 10,000 ESNPCs. A 1-week study was previously performed to evaluate the effect of cell number on survival and a dose of 10 EBs was found to elicit robust ESNPC survival and proliferation after transplantation (unpublished data). As described above, scar tissue was removed and either no treatment (control, $n = 6$), a fibrin sphere alone (Fibrin, $n = 6$), 10 EBs placed directly in the lesion site with no fibrin (10EB no Fibrin, $n = 6$), a fibrin sphere containing 10 EBs (10EB + Fibrin, $n = 8$), a fibrin sphere containing 10 EBs and HBDS with 125 ng NT-3 (Peprotech, Rock Hill, NJ), and 20 ng PDGF-AA (R&D Systems, Minneapolis, MN) (10EB + DS + GF, $n = 8$), or fibrin sphere containing 10 EBs with 125 ng NT-3 and 20 ng PDGF-AA with no HBDS (10EB + GF no DS, $n = 8$) were placed in the injury site. The untreated control group received the same surgical removal of scar tissue but no treatment with fibrin scaffolds or cells. Table 1 lists the experimental sample size for each analysis technique used in the study.

Animals were given cefazolin (15 mg/kg, twice a day) for 5 days following each surgical procedure as a prophylactic against urinary tract infections. Bladders were expressed manually twice a day until they regained bladder control, approximately 5–6 days post-initial injury. Animals with transplanted ESNPCs were immune suppressed with 10 mg/kg of cyclosporine A (Novartis, East Hanover, NJ), because mouse ESCs were being transplanted into rats. The animals were euthanized at the end of each study using an overdose of Euthasol (Virbac, France). After transcardial perfusion using 4% paraformaldehyde (Sigma), spinal cords were dissected and postfixed in 4% paraformaldehyde solution overnight. The cords were then cryoprotected in a 30% sucrose solution in phosphate-buffered saline (PBS) in preparation for frozen sections. The spinal cord was embedded in Tissue-Tek OCT compound Mounting Media (Sakura Finetek, Torence, CA) and cut into 20-µm sagittal sections using a cryostat.

Immunohistochemistry

Immunohistochemistry was used to assess the differentiation of the transplanted ESNPCs and morphological aspects of the spinal cord from each experimental group. Sections were washed with PBS and permeabilized with 0.1% Triton X-100 for 5 min. After washes in PBS, the sections were blocked with 10% bovine serum albumin (BSA, Sigma) and 2% normal goat serum (NGS, Sigma). Primary antibodies against glial fibrillary acidic

Table 1. Experimental Sample Size (N) for Each Experimental Analysis

Experimental Groups	Stereology and Differentiation Analysis (N)*	Macrophage Analysis (N)
End point	2 weeks	2 weeks
10EB no Fibrin	6	6
10EB + Fibrin	8	8
10EB + DD + GF	8	8
10EB + GF no DS	8	8
Control	—	6
Fibrin	—	6

Includes rats with no ESNPCs after 2 weeks.
*Stereology and differentiation analysis was not performed on Control and Fibrin groups because ESNPCs were not transplanted in these groups.

protein (GFAP, rabbit polyclonal, recognizing astrocytes, 1:4; ImmunoStar, Hudson, WI), neuronal class III β-tubulin (Tuj1, mouse monoclonal, recognizing neurons, 1:200; Covance Research Products, Berkeley, CA), ED1 (mouse monoclonal, recognizing macrophages/microglia, 1:100; Serotec, Oxford, UK), anti-oligodendrocyte marker O4 (O4, mouse monoclonal, recognizes oligodendrocytes, 1:200; Millipore), anti-nestin (nestin, mouse monoclonal, recognizes NPCs, 1:200; Millipore), anti-neuronal nuclei (NeuN, mouse monoclonal, recognizes mature neurons, 1:500; Millipore), and anti-SSEA-1 (SSEA-1, mouse monoclonal, recognizes mouse ESCs, 1:50; Millipore) were used to evaluate each section. Finally, appropriate secondary antibodies (Alexa Fluor 555, and 647 conjugated, 1:300; Invitrogen, Carlsbad, CA) diluted with 2% NGS were used and each section was stained with Hoechst nuclear stain (1:1000; Molecular Probes).

Stereological Analysis of Transplanted Cells

Sagittal sections of the frozen spinal cords were taken, resulting in ~100 frozen serial sections. Every 12th section was then analyzed using stereological techniques, resulting in ~8 sections from each animal being analyzed. Stereological cell counts of GFP^+ cells to determine cell survival were performed on the 12th equidistant frozen section from each animal and counterstained with the nuclear dye Hoechst. To determine the number of GFP^+ mature neurons present at the end of the 2-week study, stereological cell counts of GFP/NeuN double-positive cells was performed on the 12th equidistant frozen section from each animal. All stereological counts were performed using the Stereo Investigator Software (Version 7, MBF Biosciences, Williston, VT) and verified with a Gunderson coefficient of error less than 0.1. Animals in which ESNPCs were not seen in the spinal cord at the end of 2 weeks were included in the analysis as 0. Table 1 is a list of the experimental sample size for each analysis technique used in the study and indicates the inclusion of 0 for animals with no ESNPCs.

Differentiation Analysis of Transplanted ESNPCs

Sagittal sections of the frozen spinal cords were taken, resulting in ~100 frozen serial sections. Every 12th section was then analyzed resulting in ~8 sections from each animal being analyzed. The lesion area of every 12th serial spinal cord section was imaged at 100× magnification using an Olympus IX70 microscope (Olympus America, Melville, NY) and Magnafire Camera (Optronics, Goleta, CA). Imaging resulted in multiple 100× images per section that encompassed the entire lesion site, which were later spliced together using Photoshop (Adobe, San Jose, CA) to yield a complete picture of the lesion. To ensure accurate quantification of GFP-positive ESNPCs, control sections that did not receive cell transplants were imaged under the same conditions to account for auto fluorescence. The area of GFP^+ pixels (representing ESNPC-derived cells), and the area of pixels positive for both GFP and one of the five neural markers (Tuj1, GFAP, O4, or nestin; representing potential ESNPC-derived cell types) was measured in each section using the binary image processing software Ia32 (Leco, St. Joseph, MI) (Fig. 1). An average area across all the sections for each animal was then calculated to determine the average area of marker expression. An intensity threshold was set so that only pixels positive for the given marker were quantified within the lesion. This analysis was performed in the place of stereology because the nature of the tight organization of the transplanted cells and the markers used made delineation between adjacent cells impossible (Fig. 2). Animals in which ESNPCs were not seen in the spinal cord at the end of 2 weeks were included in the analysis as 0. Table 1 is a list of the experimental sample size for each analysis technique used in the study and indicates the inclusion of 0 for groups with no ESNPCs.

Macrophage/Microglia Profile Analysis

To assess the tissue response to the transplanted ESNPCs, the lesion area was imaged at 40× magnification and individual 40× images of the lesion area were spliced together to yield a complete picture of the lesion area and surrounding intact cord. ED1 staining of macrophages and microglia was analyzed surrounding the lesion site in six serial sections spaced 200 μm apart from each rat to evaluate the tissue response to the fibrin scaffolds. Macrophage/microglia response was analyzed by using a program written in the Matlab Image Processing Toolbox (Mathworks, Natick, MA) as described previously (17). The program allowed the user to define the lesion border based on GFAP staining. Based on this border, the program generates line profiles of a specific distance spaced 5 μm apart originating at the lesion border and preceding either rostrally or caudally from the border. The program then analyzed the pixel intensity along these lines and extracted relative ED1 fluorescence intensity as a function of distance from the glial scar border (16). The analysis yielded a profile for each sample. The ED1 intensity was normalized by a positive control from each stained section. To concisely convey these data, the normalized intensity was displayed at distances of 0, 50, 100, 200, and 400 μm rostral (−) and caudal (+) to the lesion border. In Figure 3, the −0 and +0 distance values indicate the normalized ED1 intensity directly at the border of the lesion and the adjacent spinal cord tissue both rostral (−) and caudal (+) to the lesion. The other distances, 50, 100, 200, and 400 μm

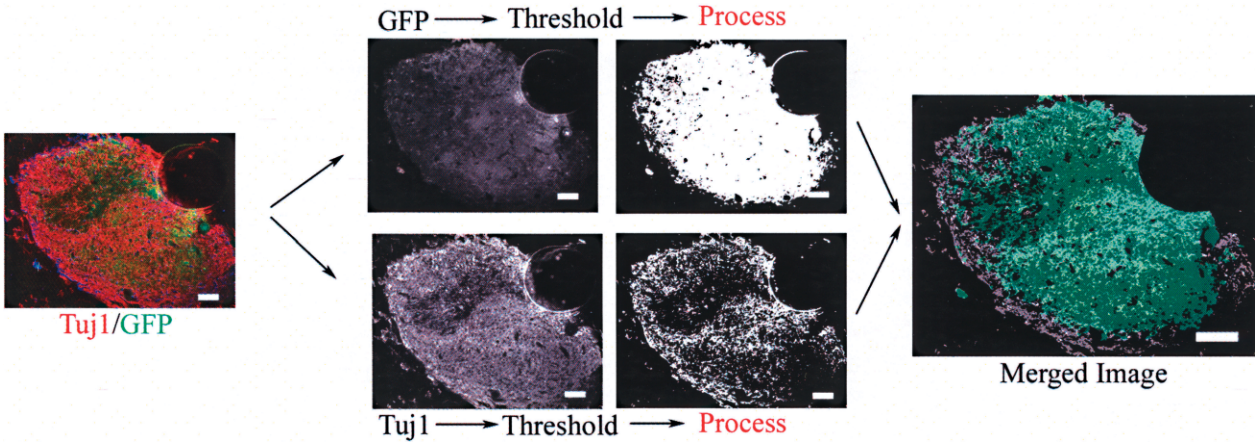

Figure 1. The figure depicts the average area of expression analysis used to analysis differentiation in the current study. Fluorescent images of transplanted ESNPCs shown here stained with β-tubulin (Tuj1, red, neurons) and green fluorescent protein (GFP, green) were taken at 10× magnification. The images were then separated into images of different colored channels (red, green, and blue) representing the different immunohistochemical stains (the red channel gives an image of Tuj1 staining and the green channel gives the picture of GFP staining). The separated images were then thresholded to identify areas that were positively stained for the given marker. The GFP image was then processed to remove any artifacts that might result in autofluorescence and thus could skew the measurement (example shown here is the edge of an air bubble in the mounting solution). The processed images were then merged using a Boolean operation that transfers those pixels that are positive for both GFP and Tuj1 into a merged image (light green pixels in merged image). The area of these pixels was then quantified to determine an area of expression of the given marker, in this case for Tuj1/GFP coexpression. Scale bar: 100 μm.

rostral (−) and caudal (+), extend out from the 0 distance. There are two 0 distance values because the injury along the rostral to caudal axis is discontinuous and thus there is a rostral value (−0) and a caudal value (+0).

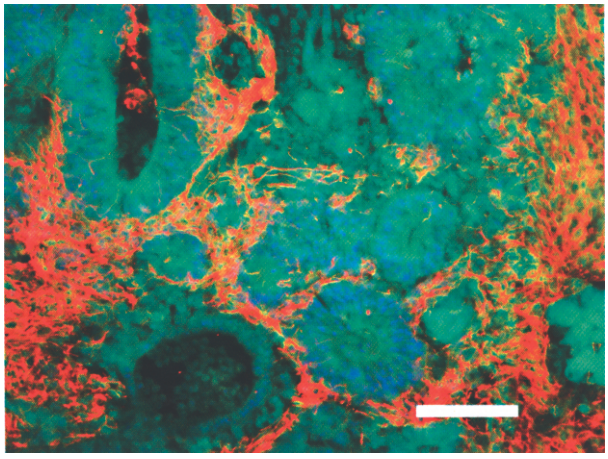

Figure 2. An image of transplanted ESNPCs after 2 weeks stained with β-tubulin III for neurons in red, GFP for transplanted ESNPCs in green, and Hoechst nuclear stain in blue. The image shows the formation of rosette-like structures within the transplanted EB that suggest early neural differentiation. The image also shows the congested nature of the transplants that makes accurate stereological counts of certain cell markers impossible. Scale bar: 100 μm.

Statistical Analysis

All statistics were performed with analysis of variance (ANOVA, planned comparison post hoc test) using Statistica (StatSoft, Tulsa, OK). Significance was determined to be $p < 0.05$. The statistical software automatically performs a Bonferroni correction for multiple comparisons.

RESULTS

Stereological Analysis of the In Vivo Survival of ESNPCs and Neuronal Differentiation

The extent of ESNPC survival at 2 weeks after transplantation depended on the method of transplantation and the presence of GF. In the 10EB no Fibrin group only 50% of the animals were found to have any GFP^+ cells present compared to 75% of the 10EB + Fibrin group, 100% of the 10EB + DS + GF group, and 89% of 10EB + GF no DS group (Table 2). The overall survival of the transplanted ESNPCs was quantified for each group using stereological counts of GFP^+ cells. There was an increase in the number of GFP^+ cells when the ESNPCs were transplanted within fibrin scaffolds with GF (10EB + DS + GF and 10EB + GF no DS) compared to the ESNPCs implanted into the lesion site alone (10EB no Fibrin, $n = 3$) and ESNPCs embedded in fibrin with no GF (10EB + Fibrin, $n = 6$) ($p < 0.05$) (Fig. 4A). The estimated number of GFP^+ ESNPCs after 2 week suggests that the transplanted cells are not only

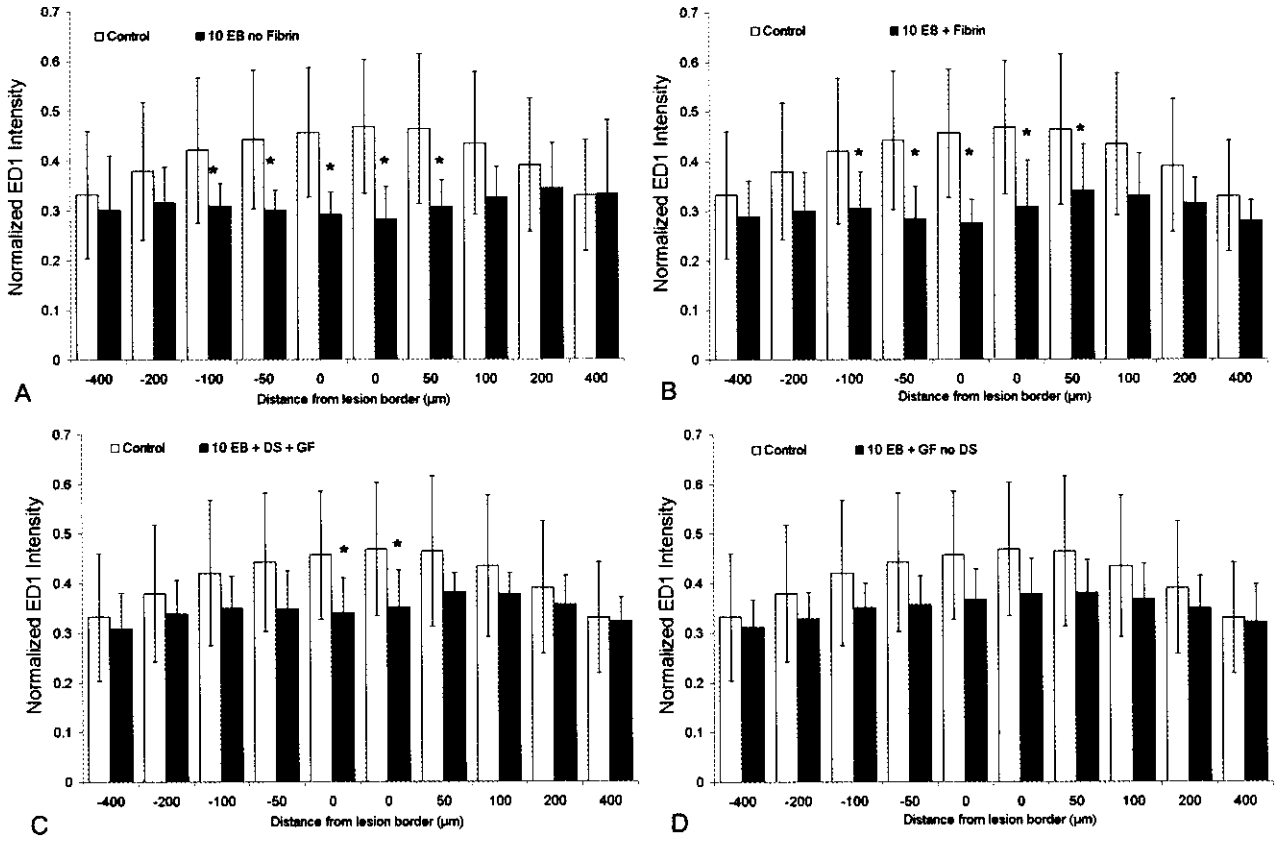

Figure 3. Effect of ESNPCs on macrophage/microglia staining. The tissue response to the ESNPCs and fibrin scaffolds containing ESNPCs was analyzed by measuring the intensity of ED1 staining as a function of distance from the lesion border. The analysis yielded an ED1 profile for each experimental group that was normalized by a positive control. (A) ED1 profile for the control (open bars, $n = 6$) and 10EB no fibrin group (filled bars, $n = 6$) 2 weeks following implantation. The normalized intensity is displayed at distances of 0, 50, 100, 200, and 400 µm rostral (−) and caudal (+) to the lesion border. The 10EB no fibrin group exhibited a significant decrease in normalized ED1 intensity at points adjacent to the lesion border ($*p > 0.05$ vs. control at same distance). (B) ED1 profile for the control (open bars, $n = 6$) and 10EB + Fibrin group (filled bars, $n = 8$) 2 weeks following implantation. The 10EB + Fibrin group exhibited a significant decrease in normalized ED1 intensity at points adjacent to the lesion border ($*p > 0.05$ vs. control at same distance). (C) ED1 profile for the control (open bars, $n = 6$) and 10EB + DS + GF group (filled bars, $n = 8$) 2 weeks following implantation. The 10EB + DS + GF group exhibited a significant decrease in normalized ED1 intensity at points immediately adjacent to the lesion border ($*p > 0.05$ vs. control at same distance). (D) ED1 profile for the control (open bars, $n = 6$) and 10EB + GF no DS group (Black bars, $n = 8$) 2 weeks following implantation. The 10EB + GF no DS group did not exhibited a significant different normalized ED1 intensity at any distance from the lesion border ($p > 0.05$). Error bars represent SD.

surviving but are proliferating. Based on the initial estimate of 1×10^5 cells per 10EBs, in the two groups without GF (10EB no Fibrin and 10EB + Fibrin) the number of cells increased twofold [$2.2 \pm 1.1 \times 10^5$ and $2.0 \pm 1.3 \times 10^5$ cells, respectively (average ± SD)] and in the two groups with GF (10EB + DS + GF and 10EB + GF no DS) the number of cells increase roughly 100fold ($12.0 \pm 6.8 \times 10^5$ and $10.0 \pm 7.8 \times 10^5$ cells, respectively).

The groups receiving ESNPCs were also stained with the neuronal nuclei marker NeuN, which identifies mature neurons. The NeuN staining revealed a population of ESNPCs that differentiated into mature neurons. The differentiation was quantified using stereological counts of the number of cells positive for NeuN and GFP (Fig. 4B). The analysis showed that the ESNPCs transplanted in fibrin scaffolds containing the HBDS and GF (10EB + DS + GF) had an increase in the number of ESNPC-derived NeuN-positive mature neurons ($p < 0.05$) (Fig. 5).

Differentiation of Transplanted ESNPCs

Due to complications associated with acquiring accurate counts of the remaining neural cell markers using stereology, a computer program was developed to quantify the expression of neural markers. The total area of pixels positive for both GFP and the marker of interest (Tuj1, GFAP, O4, nestin, or SSEA-1, staining shown in Fig. 5) was measured in every 12th section in a series of over 100 sections. The areas for each marker were

Table 2. Presence of ESNPCs in the Spinal Cord After 2 Weeks

Experimental Groups	Transplants (*N*)	ESNPCs at End Point (*N*)	With ESNPCs at End Point
10EB no Fibrin	6	3	50%
10EB + Fibrin	8	6	75%
10EB + DS + GF	8	8	100%
10EB + GF no DS	8	7	89%

then averaged for each rat. The average area of GFP expression for each experimental group was analyzed to compare this method of analysis with the stereological results of GFP^+ cells. As with the stereological data, the ESNPCs transplanted in fibrin with GF (10EB + DS + GF and 10EB + GF no DS) had greater average areas of GFP expression when compared to the ESNPCs transplanted alone (10EB no Fibrin) or the ESNPCs transplanted in fibrin without GF (10EB + Fibrin) ($p < 0.05$) (Fig. 6A). Analysis of another neuronal marker (Tuj1), using the average area of expression, showed similar trends to those observed for the stereological counts of NeuN and GFP staining. The average area of Tuj1 expression was increased for the ESNPCs in fibrin containing GF, and HBDS group (10EB + DS + GF) when compared to ESNPCs transplanted alone (10EB no Fibrin) or ESNPCs in fibrin without GF (10EB + Fibrin) ($p < 0.05$) (Fig. 6B). The average area of Tuj1 expression of the ESNPCs in fibrin containing GF with no HBDS was not significantly different from any other group.

Two markers were used to evaluate the differentiation of ESNPCs into glia. The marker O4 was analyzed to evaluate the differentiation of transplanted cells into oligodendrocytes. O4 was expressed at considerably lower levels compared to the neuronal marker Tuj1; however, there were significant difference between groups. The average area of O4 expression by ESNPC-derived cells in fibrin with GF and HBDS (10EB + DS + GF) was greater than all other groups ($p < 0.05$) (Fig. 7A). The expression of O4 by ESNPCs that were placed directly in the lesion site (10EB no Fibrin) or embedded in fibrin without GF (10EB + Fibrin) was very low. The astrocytes marker GFAP was expressed by some ESNPC-derived cells in each group. ESNPCs in fibrin with GF (10EB + DS + GF and 10EB + GF no DS) had greater average areas of GFAP expression compared to ESNPCs transplanted directly into the lesion site (10EB no Fibrin) and ESNPCs in fibrin without GF (10EB + Fibrin) ($p < 0.05$) (Fig. 7B). Finally, the expression of the NPC marker nestin was used to evaluate those ESNPCs that did not differentiate further and SSEA-1 was used to evaluate the presence of undifferentiated mouse embryonic stem cells. The average area of nestin expression did not reach the threshold for statistical significance for differences between groups; however, when compared to ESNPCs transplanted directly into the lesion site, there was a trend toward increased nestin expression for the groups with GF (10EB + DS + GF, $p = 0.056$ and

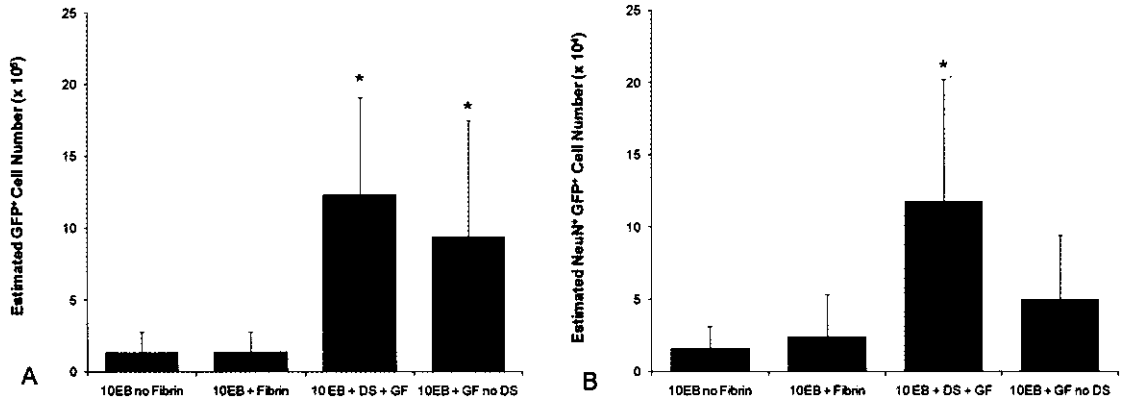

Figure 4. Stereological counts of GFP-expressing ESNPCs and GFP-expressing ESNPCs that also expressed the neuronal marker NeuN 2 weeks after transplantation. (A) A count of GFP-expressing ESNPCs was performed to analyze survival and proliferation of the transplants from each experimental group. (Note: *y*-axis is multiplied by 10^5). The ESNPCs transplanted in fibrin scaffolds containing NT-3 and PDGF (10EB + DS + GF ($n = 8$) and 10EB + GF no DS ($n = 8$)) had a significantly higher count of ESNPCs. Error bars are SD. $^*p < 0.05$ versus 10EB no Fibrin ($n = 6$) and 10EB + Fibrin ($n = 8$). (B) A count of GFP-expressing ESNPCs that also expressed the marker for mature neurons, NeuN, was performed to analyze neuronal differentiation. (Note: *y*-axis is multiplied by 10^4). The ESNPCs transplanted in fibrin scaffolds containing NT-3, PDGF, and the HBDS [10EB + GF + DS ($n = 8$)] had a significantly higher count of NeuN-positive ESNPCs when compared to ESNPCs transplanted alone (10EB no Fibrin) and ESNPCs transplanted in fibrin scaffolds alone (10EB + Fibrin). Error bars represent SD. $^*p < 0.05$ versus 10EB no Fibrin ($n = 6$) and 10EB + Fibrin ($n = 8$).

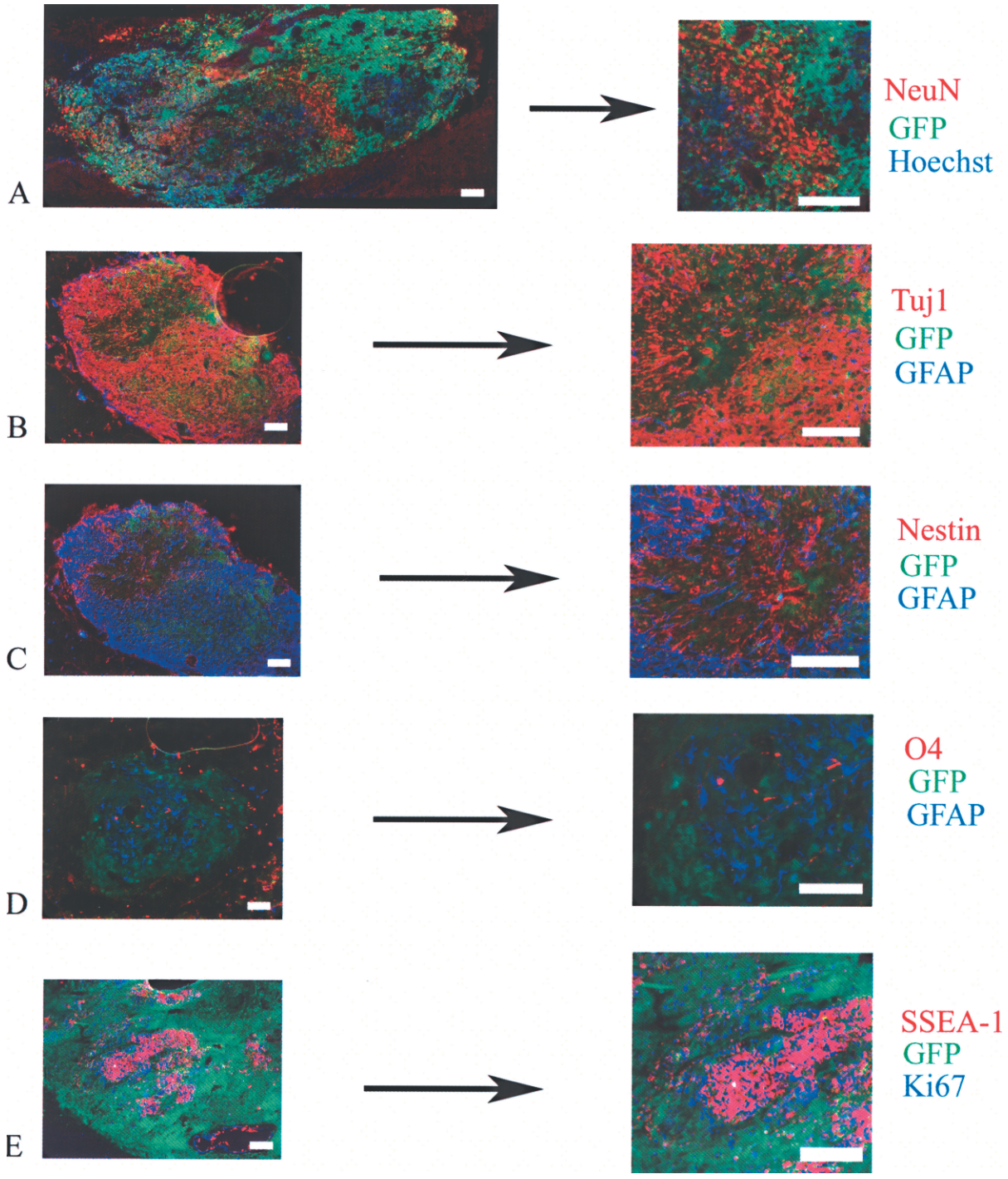

Figure 5. The figure depicts in vivo fluorescent imaging of transplanted cells 2 weeks following transplantation. (A) NeuN (red, neuronal nuclei) staining showing the expression of NeuN by transplanted cells (GFP, green) cross-stained with Hoechst nuclear stain (blue). (B) Tuj1 (red, neuronal cytoskeletal) staining showing the expression of Tuj1 by transplanted cells (GFP, green) cross-stained with GFAP (blue, astrocytes). (C) Nestin (red, ESNPC) staining showing the expression of nestin by transplanted cells (GFP, green) cross-stained with GFAP (blue, astrocytes). (D) O4 (red, early oligodendrocyte marker) staining showing the expression of O4 by transplanted cells (GFP, green) cross-stained with GFAP (blue, astrocytes). (E) SSEA-1 (red, mouse embryonic stem cell marker) staining showing the expression of SSEA-1 by transplanted cells (GFP, green) cross-stained with Ki67, the nuclear proliferation marker stain (blue). Scale bar: 100 μm.

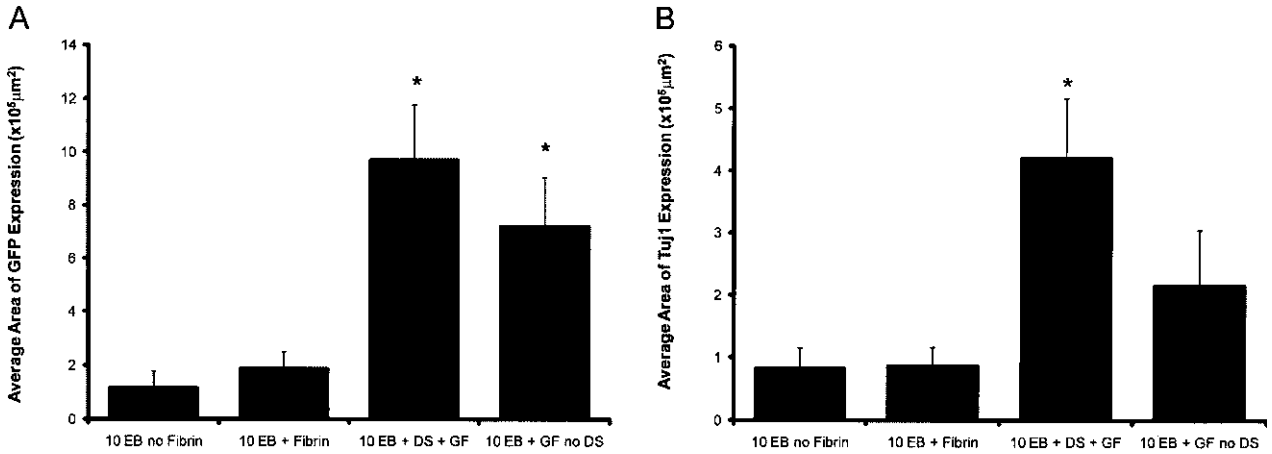

Figure 6. Average area of GFP and β-tubulin III (Tuj1) expression correlates with the stereological counts of GFP+ ESNPCs and NeuN ESNPCs. (A) The average area of GFP expression was significantly larger in groups where the ESNPCs were transplanted in fibrin scaffolds containing NT-3 and PDGF [10EB + DS + GF ($n = 8$) and 10EB + GF no DS ($n = 8$)] compared to ESNPCs transplanted alone and in fibrin scaffolds [10EB no Fibrin ($n = 6$) and 10EB + Fibrin ($n = 8$)]. Error bars are SE. *$p < 0.05$ versus. 10EB no Fibrin and 10EB + Fibrin. (B) The average area of GFP and Tuj1 coexpression was significantly larger in the group where ESNPCs were transplanted in fibrin scaffolds containing NT-3, PDGF, and the HBDS [10EB + DS + GF ($n = 8$)] when compared to the 10EB no Fibrin and 10EB + Fibrin groups. Error bars represent SEM. *$p < 0.05$ versus 10EB no Fibrin ($n = 6$) and 10EB + Fibrin ($n = 8$).

10EB + GF no DS, $p = 0.07$) (Fig. 7C). The average are of SSEA-1 expression was significantly greater when ESNPCs were transplanted in a fibrin scaffold containing the growth factors, and the HBDS when compared to all other experimental groups (10EB + DS + GF vs. 10EB + GF no DS, 10EB no Fibrin, 10EB + Fibrin, $p < 0.05$) (Fig. 7D).

Macrophage/Microglia Profile

The host reaction to an implanted material can have a significant effect on the intended function of the material. To evaluate the tissue response of the transplants, a profile of macrophage/microglia presence adjacent to the lesion site was used to assess inflammation. A program was developed that analyzed the intensity of ED1 staining as a function of distance from the lesion border. In all of the experimental groups, ED1-positive cells accumulated at the lesion border. The groups with ESNPCs transplanted directly in the lesion site (10EB no Fibrin), ESNPCS in fibrin (10EB + Fibrin), and ESNPCS in fibrin with GF and HBDS (10EB + DS + GF) exhibited a decrease in ED1 staining intensity compared to the untreated control group, immediately adjacent to the lesion border (0 µm rostral and caudal, $p < 0.05$) (Fig. 3A). There was no significant difference in ED1 intensity between the ESNPCs in fibrin with GF without HBDS (10EB + GF no DS) when compared to the untreated control ($p < 0.09$) (Fig. 3B).

DISCUSSION

The in vivo survival and differentiation of transplanted ESNPCs was evaluated in a subacute model of SCI. The transplantation of ESNPCs in fibrin scaffolds containing NT-3 and PDGF increased overall cell survival and proliferation by X-fold over 2 weeks. Furthermore, the transplantation of ESNPCs in fibrin scaffolds containing GF and HBDS increased the number of ESNPC-derived NeuN+ neurons (1.2×10^5 NeuN+ cells in the 10EB + GF + DS group compared to $<0.25 \times 10^5$ NeuN+ cells in the groups without GF). Others have found that NPC transplantation into the injured spinal cord results in poor cell survival and differentiation into a predominately glial fate (7,8,22,33). Previously, ESNPCs induced using the same 4–/4+ RA protocol were injected into a crush model of SCI 9 days after injury and found to promote a modest increase in functional recovery (21). However, the authors found that cell survival was poor (~10%), and few of the surviving cells differentiated into neurons (~8%). The findings in our current study are significant because they demonstrate the ability to enhance the survival and differentiation of NPCs into neurons after transplantation into the injured spinal cord.

ESNPCs in fibrin scaffolds containing GF exhibited robust survival and proliferation at 2 weeks following implantation into a subacute model of SCI. In vitro studies evaluating NT-3 and PDGF, at the same total doses used in this study, found that the combination resulted in increased survival of ESNPCs at 2 weeks (32). Consistent with these in vitro findings, our study found that the stereological count of ESNPCs with GF (with or without HBDS) was higher than either ESNPCs implanted directly into the lesion site or in fibrin without GF after transplantation. The stereological counts estimate that the addition of GF increased the total cell

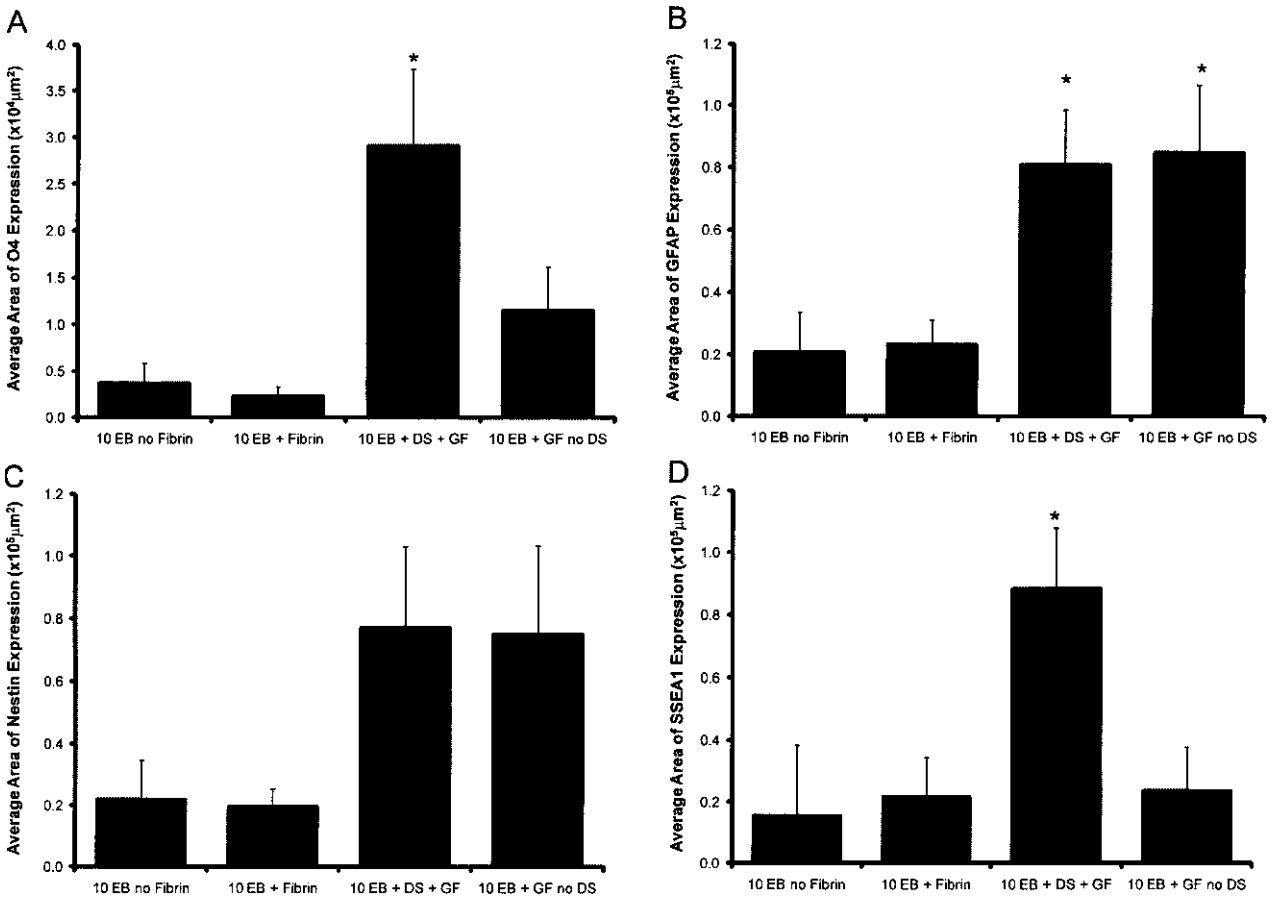

Figure 7. The conditions for ESNPC transplantation had a significant effect of differentiation. (A) The average area of GFP and O4 coexpression for ESNPCs that differentiated into oligodendrocytes was significantly increased in ESNPCs transplanted within fibrin scaffolds containing NT-3, PDGF, and the HBDS [10EB + DS + GF ($n = 8$)] compared to all other groups [$^*p < 0.05$ compared to 10EB no Fibrin ($n = 6$), 10EB + Fibrin ($n = 8$), and 10EB + GF no DS ($n = 8$)]. (B) The average area of GFP and GFAP coexpression for ESNPCs that differentiated into astrocytes was significantly increased in ESNPCs transplanted within fibrin scaffolds containing NT-3 and PDGF [10EB + DS + GF ($n = 8$) and 10EB + GF no DS ($n = 8$)] compared to ESNPCs transplanted alone and in fibrin scaffolds [10EB no Fibrin ($n = 6$) and 10EB + Fibrin ($n = 8$)] [$^*p < 0.05$ vs. 10EB no Fibrin ($n = 6$) and 10EB + Fibrin ($n = 8$)]. (C) The average area of GFP and nestin coexpression for ESNPCs remained undifferentiated was not significantly between all of the groups. (D) The average area of GFP and SSEA-1 coexpression for transplanted mouse embryonic stem cells that remained undifferentiated was significantly greater when transplanted in fibrin scaffolds containing growth factor and the HBDS when compared to all other experimental groups ($^*p < 0.05$ vs. 10EB no Fibrin, 10EB + fibrin, and 10EB + DS + GF). Error bars from all graphs represent SEM.

number approximately 10-fold over the initial estimated cell number in 2 weeks. In contrast, those ENSPCs embedded in fibrin scaffolds alone only increased roughly twofold over the same time period. Our findings are consistent with other studies that have shown that the combination of NT-3 and PDGF promotes NPC survival in models of CNS disease (14), and PDGF specifically promotes NPC proliferation (11,12).

The incorporation of the HBDS in fibrin scaffolds containing GF and ESNPCs resulted in an increase in the number of ENSPC-derived $NeuN^+$ cells. These findings are consistent with in vitro studies that found NT-3 and PDGF delivered from the HBDS increased the percentage ESNPCs that differentiated into neurons (32). It has been shown that soluble NT-3 promotes the differentiation of human ESCs into neurons in culture and treatment of NPCs with NT-3 results in the formation of bipolar neurons (19,20). The stereological count of $NeuN^+$ neurons derived from ESNPCs in fibrin with GF and no HBDS was not different from the other groups. These results suggest that controlled delivery of NT-3 and PDGF using the HBDS was required for the increase in neuronal differentiation compared groups without GF.

The addition of the HBDS could have affected the differentiation of the ESNPCs. Heparin alone in the cul-

ture medium of ESCs and NPCs has been shown to increase proliferation through secondary interactions with fibroblast growth factor (FGF) that enhance FGF's mitotic activity (5,15). Willerth et al. found that using the same concentration of heparin found in the HBDS resulted in a decrease in astrocytes differentiation (32). In our study, the HBDS had no effect on astrocytes differentiation of ESNPCs, and thus it is unlikely that direct interaction between heparin and the ESNPCs resulted in an increase in $NeuN^+$ neurons.

As with heparin, the presence of the heparin-binding peptide from the HBDS could have an effect on ESNPCs differentiation. Others have demonstrated the ability of cell adhesion sequences from laminin to promote differentiation of NPCs (28). However, evaluation of the HBDS in vitro showed that the affinity peptide alone in culture had no effect on neuronal differentiation (32). Based on these previous results, it is unlikely that interaction of ESNPCs with the heparin-binding peptide in the HBDS accounted for the increase in $NeuN^+$ neurons. A more likely explanation for the observed increase in $NeuN^+$ neurons with the HBDS is its ability to sequester NT-3 and PDGF to the fibrin scaffold (29,32). Furthermore, the HBDS could also have increased the residence time of other endogenously produced GFs within the fibrin scaffolds.

A method to analyze the differentiation of transplanted ESNPCs was developed to compliment the stereological analysis performed in this study. With the exception of NeuN, the cell differentiation markers used in this study were cell surface (SSEA-1/O4) or intracellular proteins (nestin, Tuj1, GFAP) that are expressed in different locations within the cell. As a consequence, if the cell of interest is adjoining another cell with the same marker it is difficult to delineate the boundary between each independent cell and thus impossible to make an accurate stereological count. A program was written that evaluates the total area of pixels that are positive for both green fluorescent protein (GFP) and the neural marker of interest. While this method of analysis does not indicate a specific number of cells stained positive for a given marker, it does quantify the average area of expression for each given marker. The area of expression can then be compared between experimental groups to determine a difference in expression between groups. To assure that the method correlated to the stereological counts of the GFP^+ and $NeuN^+$ cells, we analyzed the amount of GFP expression for transplanted ESNPCs and Tuj1 for neurons. The analysis of average area of expression for GFP and Tuj1 predicted the same trends obtained with the stereological counts for transplanted ESNPCs that expressed the neuronal marker NeuN and GFP; thus, for a given marker a greater area of expression correlated with a greater number of cells, as expected. However, this method does not allow correlations between markers (e.g., area of Tuj1 vs. GFAP) that could be performed with absolute cell number counts from stereology.

By analyzing the average area of GFP^+ O4 expression using this method, we found that ESNPC-derived cells in fibrin with GF and the HBDS showed increased O4 expression compared to all other groups. The combination of the two GF and the HBDS was found to increase oligodendrocyte differentiation in vitro ESNPCs (32). The increased O4 expression seen in the 10EB + DS + GF group suggests that the presence of the controlled delivery of GF promotes oligodendrocyte differentiation. ESNPCs in fibrin containing GF with or without HBDS showed an increase in the average area of GFAP expression compared to groups without GF. In vitro studies found that the addition of the HBDS decreased astrocytes differentiation compared to controls that were cultured without the GF (32). While the addition of the GF resulted in increased GFAP and O4 staining, the neuronal markers were more widely expressed than glial markers on ESNPC-derived cells after transplantation.

Staining with the mouse ESC marker SSEA-1 revealed a moderate amount of expression of the ESC marker by the transplanted cells. This is not surprising considering the RA induction protocol only results in a population of cells that are 70% nestin-positive ESNPCs (31). Quantification of the average area of SSEA-1 expression revealed differences between experimental groups. The 10EB + DS + GF group average are of SSEA-1 expression was greater than all other experimental groups. Previously, it has been shown that PDGF can enhance the survival and proliferation of SSEA-1-positive mouse ESCs in in vitro culture (31). It follows that in this study the presence of the growth factors and the HBDS enhanced the survival and proliferation of SSEA-1-positive mouse ESCs.

Analysis of the average area of marker expression is not the same as stereological counts of cells. As mentioned above, the quantification of proteins that are located in different places within the cell make comparison of areas between different antibodies inaccurate (e.g., area positive for Tuj1 vs. GFAP). Likewise, the summation of the different average areas of expression (Tuj1, GFAP, nestin, and SSEA-1) are not expected to add up to the average area of expression of GFP^+ transplanted ESNPCs and they do not. It is possible that the differences in area are a result of the quantification method and it is possible that some of the GFP^+ cells are expressing markers other than those assayed in this study. Based on the type of analysis that was utilized in this study, it is impossible to tell. However, the goal of the analysis was to look at the differential effects these growth factors have on differentiation of the ESNPCs

into the three neural subtypes (neurons, oligodendrocytes, and astrocytes). The foreign body response to a transplanted material can drastically affect the function of the material in vivo. We analyzed the intensity of macrophage/microglia staining surrounding the implants assess any adverse response to the ESNPC containing scaffolds. In previous studies, we have found that fibrin scaffolds alone do not induce an adverse response in the surrounding host tissue based on the presence of macrophage/microglia (17). In this study we found that three of the four groups that were treated with ESNPCs had a decrease in the intensity of macrophage staining surrounding the lesion site compared to the control group (received the same surgical procedures but no treatment). Transplanted NPCs have been found to be neuroprotective and increase the viability of neural tissue during and following injury to the CNS (1). Similarly, if the transplanted ESNPCs increase survival of host tissue, then that may have led to the decrease in macrophage/microglia staining surrounding the lesion.

CONCLUSIONS

Here we have investigated the feasibility of transplanting ESNPCs within fibrin scaffolds containing GF and a HBDS to increase cell survival and direct their differentiation following transplantation into the injured spinal cord. Transplantation of the ESNPCs in fibrin scaffolds containing NT-3 and PDGF enhanced their survival and proliferation 2 weeks after transplantation. Also, the addition of a HBDS resulted in an increase in the number of ESNPCs that differentiated into $NeuN^+$ neurons. These results are the first step toward a larger goal of enhancing functional recovery following SCI by repopulating the damaged cord with neurons and oligodendrocytes that can increase local plasticity. Finally, the method of implantation outlined in this work could be used to increase the survival and differentiation of transplanted cells for other cell therapies.

ACKNOWLEDGMENTS: This study was supported by NIH RO1 NS051454. The authors thank Dan Hunter and Dr. Susan Mackinnon for the use of their cryostat and stereology equipment.

REFERENCES

1. Aharonowiz, M.; Einstein, O.; Fainstein, N.; Lassmann, H.; Reubinoff, B.; Ben-Hur, T. Neuroprotective effect of transplanted human embryonic stem cell-derived neural precursors in an animal model of multiple sclerosis. PLoS ONE 3(9):e3145; 2008.
2. Bain, G.; Kitchens, D.; Yao, M.; Huettner, J. E.; Gottlieb, D. I. Embryonic stem cells express neuronal properties in vitro. Dev. Biol. 168(2):342–357; 1995.
3. Bareyre, F. M. Neuronal repair and replacement in spinal cord injury. J. Neurol. Sci. 265(1–2):63–72; 2008.
4. Bareyre, F. M.; Kerschensteiner, M.; Raineteau, O.; Mettenleiter, T. C.; Weinmann, O.; Schwab, M. E. The injured spinal cord spontaneously forms a new intraspinal circuit in adult rats. Nat. Neurosci. 7(3):269–277; 2004.
5. Caldwell, M. A.; Svendsen, C. N. Heparin, but not other proteoglycans potentiates the mitogenic effects of FGF-2 on mesencephalic precursor cells. Exp. Neurol. 152(1):1–10; 1998.
6. Cao, Q. L.; Howard, R. M.; Dennison, J. B.; Whittemore, S. R. Differentiation of engrafted neuronal-restricted precursor cells is inhibited in the traumatically injured spinal cord. Exp. Neurol. 177(2):349–359; 2002.
7. Cao, Q. L.; Zhang, Y. P.; Howard, R. M.; Walters, W. M.; Tsoulfas, P.; Whittemore, S. R. Pluripotent stem cells engrafted into the normal or lesioned adult rat spinal cord are restricted to a glial lineage. Exp. Neurol. 167(1):48–58; 2001.
8. Chow, S. Y.; Moul, J.; Tobias, C. A.; Himes, B. T.; Liu, Y.; Obrocka, M.; Hodge, L.; Tessler, A.; Fischer, I. Characterization and intraspinal grafting of EGF/bFGF-dependent neurospheres derived from embryonic rat spinal cord. Brain Res. 874(2):87–106; 2000.
9. Courtine, G.; Song, B.; Roy, R. R.; Zhong, H.; Herrmann, J. E.; Ao, Y.; Qi, J.; Edgerton, V. R.; Sofroniew, M. V. Recovery of supraspinal control of stepping via indirect propriospinal relay connections after spinal cord injury. Nat. Med. 14(1):69–74; 2008.
10. Eriksson, P. S.; Perfilieva, E.; Bjork-Eriksson, T.; Alborn, A. M.; Nordborg, C.; Peterson, D. A.; Gage, F. H. Neurogenesis in the adult human hippocampus. Nat. Med. 4(11): 1313–1317; 1998.
11. Erlandsson, A.; Brannvall, K.; Gustafsdottir, S.; Westermark, B.; Forsberg-Nilsson, K. Autocrine/paracrine platelet-derived growth factor regulates proliferation of neural progenitor cells. Cancer Res. 66(16):8042–8048; 2006.
12. Erlandsson, A.; Enarsson, M.; Forsberg-Nilsson, K. Immature neurons from CNS stem cells proliferate in response to platelet-derived growth factor. J. Neurosci. 21(10):3483–3491; 2001.
13. Fawcett, J. W.; Asher, R. A. The glial scar and central nervous system repair. Brain Res. Bull. 49(6):377–391; 1999.
14. Fressinaud, C. Repeated injuries dramatically affect cells of the oligodendrocyte lineage: Effects of PDGF and NT-3 in vitro. Glia 49(4):555–566; 2005.
15. Furue, M. K.; Na, J.; Jackson, J. P.; Okamoto, T.; Jones, M.; Baker, D.; Hata, R.; Moore, H. D.; Sato, J. D.; Andrews, P. W. Heparin promotes the growth of human embryonic stem cells in a defined serum-free medium. Proc. Natl. Acad. Sci. USA 105(36):13409–13414; 2008.
16. Jain, A.; Kim, Y. T.; McKeon, R. J.; Bellamkonda, R. V. In situ gelling hydrogels for conformal repair of spinal cord defects, and local delivery of BDNF after spinal cord injury. Biomaterials 27(3):497–504; 2006.
17. Johnson, P. J.; Parker, S. R.; Sakiyama-Elbert, S. E. Fibrin-based tissue engineering scaffolds enhance neural fiber sprouting and delay the accumulation of reactive astrocytes at the lesion in a subacute model of spinal cord injury. J. Biomed. Mater. Res. 92A:152–163; 2010.
18. Karimi-Abdolrezaee, S.; Eftekharpour, E.; Wang, J.; Morshead, C. M.; Fehlings, M. G. Delayed transplantation of adult neural precursor cells promotes remyelination and functional neurological recovery after spinal cord injury. J. Neurosci. 26(13):3377–3389; 2006.
19. Lachyankar, M. B.; Condon, P. J.; Quesenberry, P. J.; Litofsky, N. S.; Recht, L. D.; Ross, A. H. Embryonic precursor cells that express Trk receptors: Induction of different cell fates by NGF, BDNF, NT-3, and CNTF. Exp. Neurol. 144(2):350–360; 1997.
20. Levenberg, S.; Burdick, J. A.; Kraehenbuehl, T.; Langer,

R. Neurotrophin-induced differentiation of human embryonic stem cells on three-dimensional polymeric scaffolds. Tissue Eng. 11(3–4):506–512; 2005.
21. McDonald, J. W.; Liu, X. Z.; Qu, Y.; Liu, S.; Mickey, S. K.; Turetsky, D.; Gottlieb, D. I.; Choi, D. W. Transplanted embryonic stem cells survive, differentiate and promote recovery in injured rat spinal cord. Nat. Med. 5(12):1410–1412; 1999.
22. McDonald, J. W.; Sadowsky, C. Spinal-cord injury. Lancet 359(9304):417–425; 2002.
23. McKeon, R. J.; Schreiber, R. C.; Rudge, J. S.; Silver, J. Reduction of neurite outgrowth in a model of glial scarring following CNS injury is correlated with the expression of inhibitory molecules on reactive astrocytes. J. Neurosci. 11(11):3398–3411; 1991.
24. Morshead, C. M.; Reynolds, B. A.; Craig, C. G.; McBurney, M. W.; Staines, W. A.; Morassutti, D.; Weiss, S.; van der Kooy, D. Neural stem cells in the adult mammalian forebrain: A relatively quiescent subpopulation of subependymal cells. Neuron 13(5):1071–1082; 1994.
25. Nakamura, M.; Okano, H.; Toyama, Y.; Dai, H. N.; Finn, T. P.; Bregman, B. S. Transplantation of embryonic spinal cord-derived neurospheres support growth of supraspinal projections and functional recovery after spinal cord injury in the neonatal rat. J. Neurosci. Res. 81(4):457–468; 2005.
26. Rudge, J. S.; Silver, J. Inhibition of neurite outgrowth on astroglial scars in vitro. J. Neurosci. 10(11):3594–3603; 1990.
27. Sakiyama-Elbert, S. E.; Hubbell, J. A. Development of fibrin derivatives for controlled release of heparin-binding growth factors. J. Control. Release 65(3):389–402; 2000.
28. Silva, G. A.; Czeisler, C.; Niece, K. L.; Beniash, E.; Harrington, D. A.; Kessler, J. A.; Stupp, S. I. Selective differentiation of neural progenitor cells by high-epitope density nanofibers. Science 303(5662):1352–1355; 2004.
29. Taylor, S. J.; Rosenzweig, E. S.; McDonald, 3rd, J. W.; Sakiyama-Elbert, S. E. Delivery of neurotrophin-3 from fibrin enhances neuronal fiber sprouting after spinal cord injury. J. Control. Release 113(3):226–235; 2006.
30. Willerth, S. M.; Arendas, K. J.; Gottlieb, D. I.; Sakiyama-Elbert, S. E. Optimization of fibrin scaffolds for differentiation of murine embryonic stem cells into neural lineage cells. Biomaterials 27(36):5990–6003; 2006.
31. Willerth, S. M.; Faxel, T. E.; Gottlieb, D. I.; Sakiyama-Elbert, S. E. The effects of soluble growth factors on embryonic stem cell differentiation inside of fibrin scaffolds. Stem Cells 25(9):2235–2244; 2007.
32. Willerth, S. M.; Rader, A.; Sakiyama-Elbert, S. E. The effect of controlled growth factor delivery on embryonic stem cell differentiation inside fibrin scaffolds. Stem Cell Res. 1:205–218; 2008.
33. Zahir, T.; Nomura, H.; Guo, X. D.; Kim, H.; Tator, C.; Morshead, C.; Shoichet, M. Bioengineering neural stem/progenitor cell-coated tubes for spinal cord injury repair. Cell Transplant. 17(3):245–254; 2008.